

Determining the Curie and Néel Temperature of Minerals

Carolyn Pickler, Neil Edelman

April 13, 2007

Abstract

The Curie and Néel temperature are the temperatures at which a magnetic material becomes paramagnetic; hence losing its magnetic properties. By heating mineral samples of pyrrhotite ($Fe_{1-x}S$) and magnetite (Fe_3O_4) in the presence of a solenoid induced magnetic field, we were able to determine the Néel and Curie temperatures. The Néel temperature of pyrrhotite, an antiferromagnetic mineral, was determined to be $597 \pm 2K$, which agrees with the theoretical value of $598K$. While attempting to measure the Curie temperature of magnetite, a ferrimagnetic mineral, one of the heating coils broke resulting in the ending of our experiment. Since no change in magnetic properties was observed in our collected data, we can only assume that the Curie temperature occurs at a value greater than that at which the catastrophic event occurred, $702 \pm 3K$. This value agrees with the theoretical one of $851 K$.

1 Introduction

In today's society magnetic materials prove to be extremely useful. They have a wide range of applications, from the construction of audio speakers and motors to computer hard disks and videotapes [1]. To better understand these materials, we study the minerals that make them up. In our case, we'll study magnetite, (Fe_3O_4), and pyrrhotite, ($Fe_{1-x}S$).

Pyrrhotite is an antiferromagnetic mineral. The spins of the electrons align in a regular pattern with the neighboring ones, which are pointing in opposite directions. The magnetic susceptibility of antiferromagnetic materials changes with temperature. At low temperature, it is diamagnetic, which means that it displays magnetic properties only in the presence of a magnetic field and is caused by changes in the orbital motion of the electrons. [2].

Pyrrhotite is an iron sulphide, which displays two symmetries, hexagonal and monoclinic. The displayed symmetry depends on the concentration of sulphur in the mineral. When there is a small amount of sulphur, its symmetry is closer to hexagonal while having larger amounts of sulphur indicates monoclinic symmetry. It is weakly magnetic and after magnetite, it is the most common magnetic mineral [3]. Its uses include being a source of sulphur and an iron

ore [4]. Our sample of pyrrhotite comes from a mine in the Sudbury area. It is known to contain some nickel, which could affect the measured Curie temperature and account for any systematic error.

Magnetite is a ferrimagnetic mineral. It possesses the same properties as a ferromagnetic mineral except instead of parallel alignment of the dipoles, it has anti-parallel alignment of unequal spins [5]. Once exposed to a magnetic field, it remains magnetized even when the field is removed [6]. Of all the magnetic minerals, it displays the strongest magnetism [7]. This mineral is important to us since it is a major iron ore, which is used by the oil industry [8].

When these minerals are subject to increasing temperatures, there is an increase in thermal agitation. This increase means that there is a decrease in the effectiveness of the dipole alignment for magnetite and pyrrhotite becomes more and more disordered. When the temperature is great enough, it will break the dipole alignment of magnetite, which results in the mineral becoming paramagnetic. This temperature is referred to as the Curie temperature [9]. At this temperature, the magnetite atoms will only react with each other when a magnetic field is present, meaning it is paramagnetic. Paramagnetic materials are commonly considered non-magnetic because of their extremely weak magnetism. For pyrrhotite, once the temperature is great enough, it will also become paramagnetic. This temperature is referred to as the Néel temperature. At this temperature, the thermal energy is great enough to destroy the magnetic ordering within the mineral [2]. For both minerals, once the temperature has decreased below their Curie or Néel temperature, they will regain their ferromagnetic (magnetite) and diamagnetic (pyrrhotite) properties.

Each mineral will be magnetized once exposed the magnetic field. The magnetic permeability of the mineral can be determined by examining the ratio of the amplitude of magnetic field of air and that of the mineral. This ratio will be equal to the magnetic susceptibility plus one [10].

$$\frac{B_s}{B_a} = \chi + 1 \quad (1)$$

where B_s is the sample, B_a is the reference coil, which is air; χ is the magnetic susceptibility.

While increasing the temperature of the mineral as it is being subjected to a magnetic field, magnetic hysteresis

will be observed. Hysteresis is the delayed effect in a material's magnetization when the external magnetic field is changed. This results in a curve, referred to as the hysteresis curve. It is the graph of the relationship between the magnetic field and the magnetic flux density. This curve results in a point, magnetic saturation, where an increase in the magnetic field will no longer result in a change in flux density [11].

The magnetic field applied to the sample was generated using a solenoid. By tightly winding a coil around a cylinder and passing a current through it, a magnetic field is generated. This is referred to a solenoid. The magnetic field of a solenoid is determined by the following equation, assuming it is ideal.

$$B = (\mu) * N * I \quad (2)$$

where B is the magnetic field, N is the number of turns of the coil per unit length, I is the current, and μ_0 is the permeability constant, whose value is,

$$4\pi \times 10^{-7} TmA^{-1} \quad (3)$$

[12]

EMF stands for electromotive force and is defined as the amount of energy per uni charge that is reversibly converted to form electrical energy. The EMF of the solenoid can defined by the following equation.

$$emf = -N \frac{d\Phi}{dt} \quad (4)$$

where i is the current, t is the time, and N is the number of turns per unit length [13].

We passed our signal though the Fourier transform and calculated the frequency response. Given a signal with finite energy $f(t)$, we define its Fourier transform $F(\omega)$ by

$$F(\omega) = \int_{-\infty}^{\infty} f(t)e^{-j\omega t} dt \quad (5)$$

Here $|F(\omega)|$ is called the magnitude spectrum of $f(t)$ [14].

2 Experimental Methods

When proposing the experiment, we planned to use the ballistic method to determine the Curie and Néel temperatures. This method involves crushing the sample and packing it tightly into a cylindrical vessel and then projected it through a uniform magnetic field. This method was abandoned due to size restriction. The sample must be large with respect to the coil but the field must be large with respect to the sample.

After abandoning the ballistic method, we planned to use a rotating coil to accomplish the measurements. This

method was abandoned due to the size and complexity of the set-up. In order to get a good signal, the coils would have had to rotate fast. Since the coils are rotating, a limited number of rotations would be required. The size of the cavity in which the sample would be rotating must be small in comparison to the size of the sample.

Finally, we came upon the idea of using an alternating field. During the design of the rotating coil system, it appeared to be slightly less complex to rotate the 'fixed' electromagnet. This would allow a fixed sensed coil, which would reduce the space required. It was observed that this could be further simplified by making the driving the electromagnet with an alternating coil. Due to the large inductance of the solenoid, a large voltage is required to drive the current through. Since the inductance of the solenoid is large and,

$$V = L \frac{di}{dt} \quad (6)$$

we require a large voltage to be applied to the solenoid [9]. Using AC, direct from the wall outlet, we saw that this produced a very poor approximation to a sinusoidal signal. To provide adequate current of both polarities, a push-pull transistor amplifier would be required, however neither matched PNP/NPN nor matched N-channel/P-channel MOSFETs were available. Both of these issues were resolved by having a single polarity amplifier driving a step-up transformer. While this is very inefficient, due to the DC component of the current through the transformer, it got the job done. The mineral was crushed up, to pieces no smaller than 0.5 mm. This was to ensure that the sample wasn't destroyed and we'd still be able to measure the Curie/Néel temperature [15]. The crushed sample was placed inside a cylindrical vessel. It filled up to and including the area that comprised the first sensing coil. The area that comprised the second sensing coil was left empty. This allowed us to compare between the magnetization of the sample and that of air, which was used as our reference. This cylindrical vessel was inserted into a solenoid of 2500 turns, which was connected to our circuit that provided the AC current.

The set-up is seen in Figure 1.

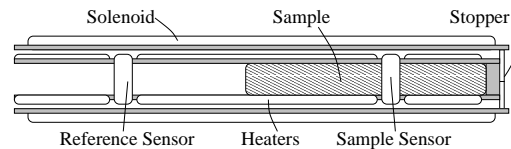


Figure 1: The set-up of the experiment.

The set-up open-circuited on us during the calculation of magnetite's Curie temperature. We noticed a bubble in the heater circuit after the explosion; this was probably the preceding factor. A heating coil wire was broken off, that

caused the power-supplies to go from supplying a $42W$ to $0W$, causing a catastrophic meltdown in the current. Originally, we had planned to use Hematite (Fe_2O_3), but the coil was unusable after this event.

In the room where this experiment was performed, the magnetic field of the Earth was measured to be -4.4 ± 0.1 mT; this was not taken into account because it was negligible.

Resonant frequency of the heating coil was $75kHz$. We calibrated our equipment using this data to $65kHz$. The hardware we used (*LabMaster*[16]) took -2048 to 2047 steps of current, corrected for Volts experementally. We only used 120 of those steps, since the calibration revealed that the signal appoched saturation. The signal was offset to get the sinusoid's zero position, $\sin 0$, which equals the zero position for our signal.

3 Results and Discussion

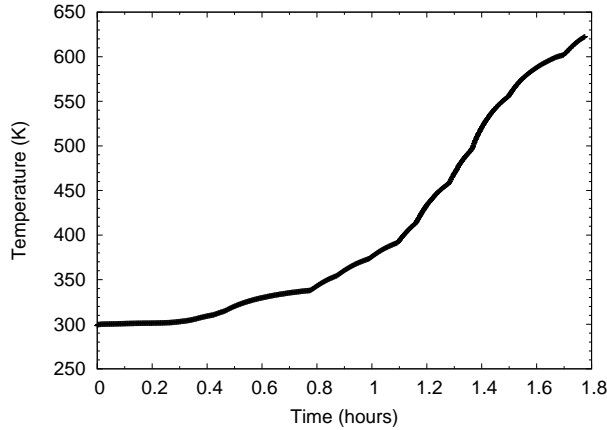


Figure 2: Temperature vs time for pyrrhotite.

As time progressed, the temperature was increased as seen in Figure 2. This increase in temperature resulted in our sample being coated with a blue mineral. This mineral is thought to be bornite, which a copper sulphide that is commonly found with pyrrhotite. With more time, the sample could be analysed to be certain.

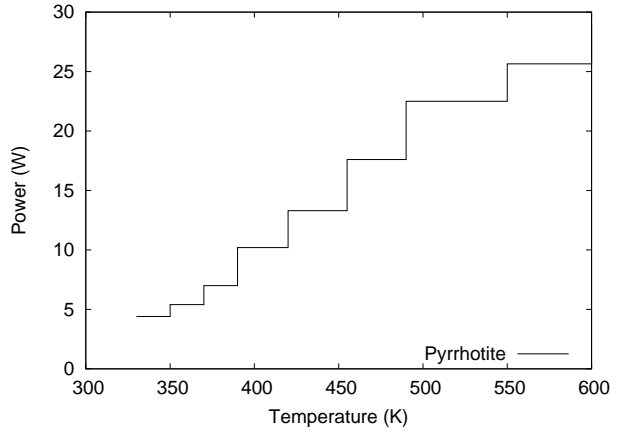


Figure 3: Power vs temperature for pyrrhotite.

The power was increased over the course of the experiment as seen in Figure 3 and as it increased, its derivative is quantised. We would only increase the power when the temperature was increasing by less than 4 demi-degrees celsius per minute.

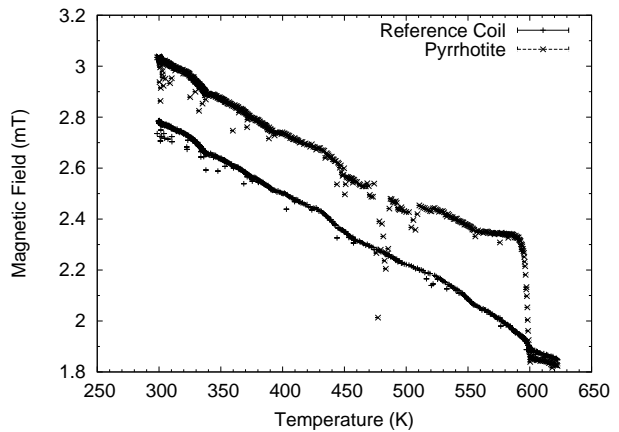


Figure 4: Magnetic field vs temperature for pyrrhotite.

The mineral becomes paramagnetic once the Néel temperature is reached. As seen in Figure 4, that the temperature at which this change in magnetism occurs is at $595 \pm 5K$.

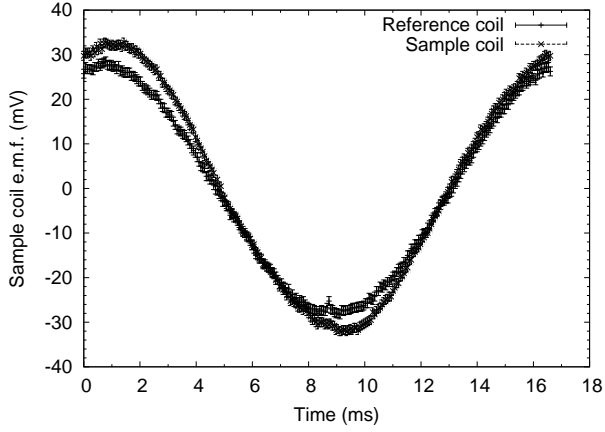


Figure 5: Hysteresis of voltage vs time for pyrrhotite.

We can see in Figure 5 a snapshot of the largest non-linearity seen in Figure 4, which occurs at approximately $570K$. This allows us to see the sample's voltage as a function of time. We want to take the ratio of the sample with respect to the reference to obtain Figure 6.

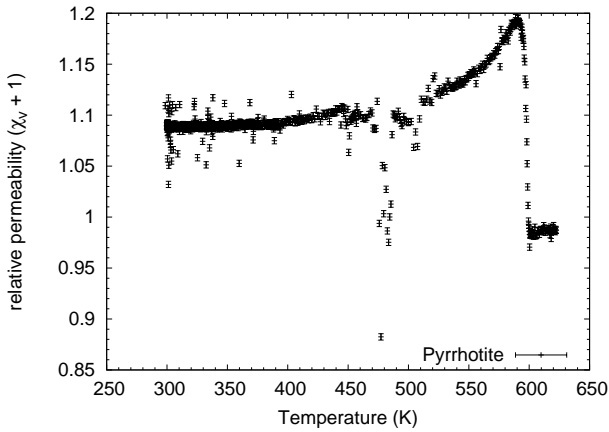


Figure 6: $\chi_{pyrrhotite}$ vs temperature for pyrrhotite.

Figure 6 provides a more accurate measurement of pyrrhotite's Néel temperature because it allows us to more closely examine the behaviour of the sample. This can be explained by the fact that by taking the ratio, the reference will cancel out the background noise, which is any external variations in the field not caused by the sample. When taking the ratio of the sample and reference, we get the one plus the magnetisation. The Néel temperature was found to be $595 \pm 5K$. The temperature was found at before the peak of pyrrhotite, an antiferromagnetic mineral, assuming anisotropy, which means the atoms are arranged in regular lattices [17].

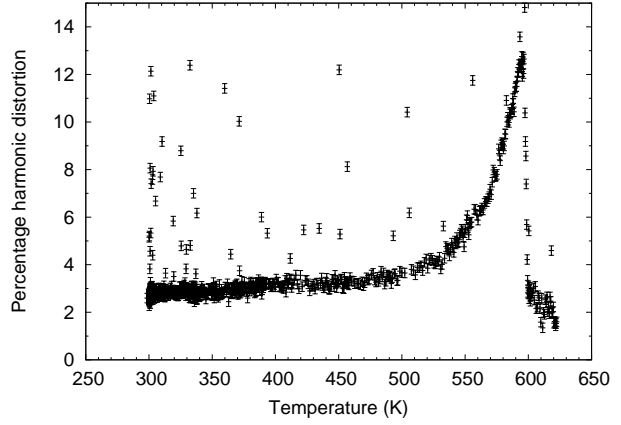


Figure 7: Harmonic distortion for pyrrhotite.

Harmonic distortion is the observed non-linearity. Figure 7 allows us to see the harmonic distortion, which is proportional to the hysteresis, as a function of temperature. The peak in harmonic distortion will occur at the Néel temperature, which shows a high degree of precision because it is over a larger range than the magnetic permeability. From Figure 7, we found the Néel temperature to be $597 \pm 2K$.

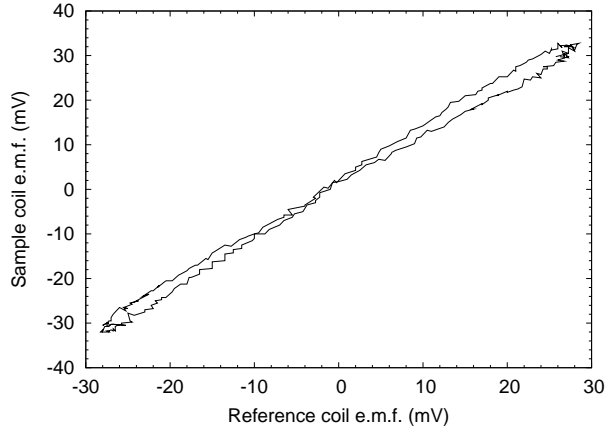


Figure 8: Hysteresis of the EMF for pyrrhotite.

Using the same data as Figure 5, we were able to plot to see the EMF hysteresis of the sample.

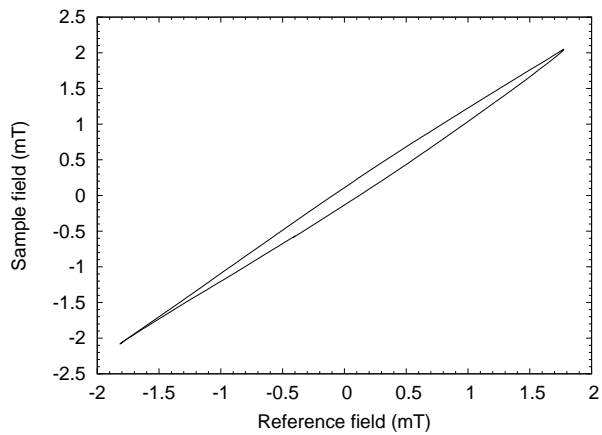


Figure 9: Hysteresis of the magnetic field for pyrrhotite.

Figure 9 is the integral of Figure 8. This allows us to see the magnetic hysteresis of the sample at $570K$. The next sample to be analysed was magnetite.

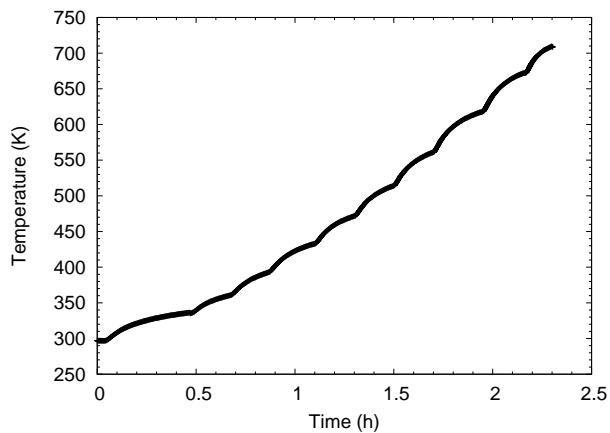


Figure 10: Temperature vs time for magnetite.

As seen in Figure 10, the temperature was increased over time. This increase suddenly stopped at approximately $700K$ when a catastrophic event occurred; one of the heating coils broke. We can no longer make any further measurements.

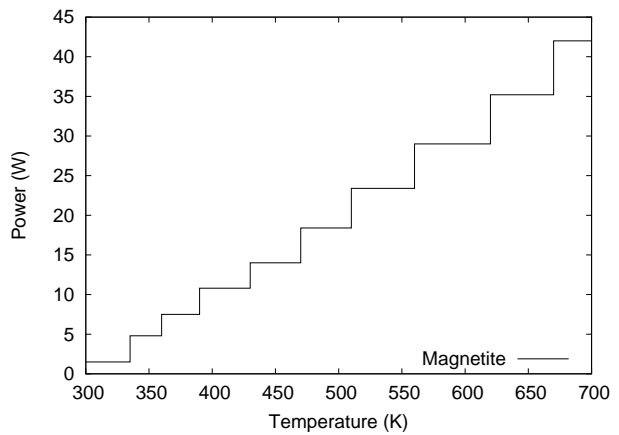


Figure 11: Power vs temperature for magnetite.

Figure 11 shows that as the temperature increases, which it did over time, so did the power which was applied by us. As with pyrrhotite, the derivative is quantised as the temperature increases.

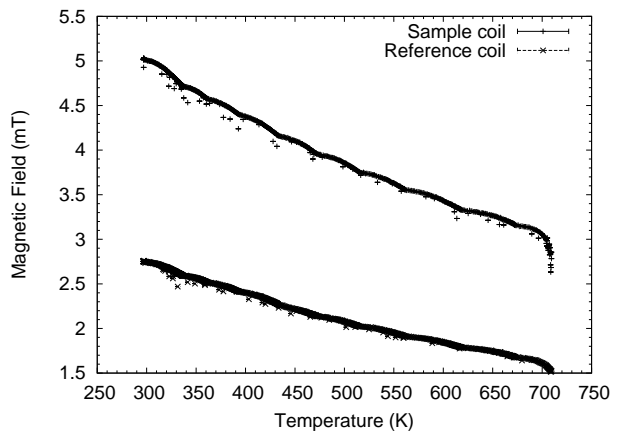


Figure 12: Magnetic field vs temperature for magnetite.

By examining Figure 12, we can see that the magnetism did not undergo any drastic changes during the elapsed time before the catastrophic event. This brings us to the conclusion that the Curie temperature must occur at a value greater than $690 \pm 10K$, which is temperature at which measurement of the magnetic field halted.

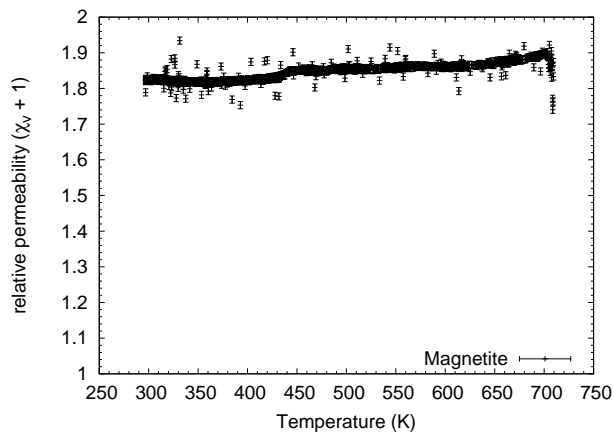


Figure 13: $\chi_{magnetite}$ vs temperature for magnetite.

Figure 13 puts the sample in ratio with the reference. As with Figure 12, we do not see any drastic changes in the magnetism during the elapsed time. This means that the Curie temperature was not obtained because at this temperature, the ferrimagnetic mineral would become paramagnetic. This change in magnetic permeability would result in a drastic change in magnetisation, which would be observed in Figure 13. From this Figure 13, we can only conclude that its Curie temperature is greater than $702 \pm 3K$.

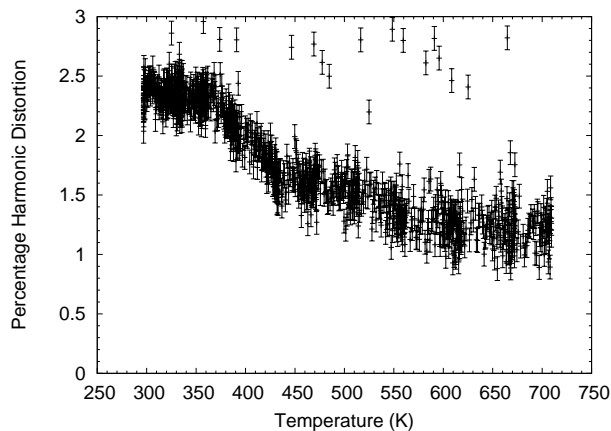


Figure 14: Harmonic distortion for magnetite.

Figure 14 does not clearly display the catastrophic event. We must keep in mind that the harmonic distortion is approximately proportional to the hysteresis of the mineral, in this case magnetite. When the harmonic distortion reaches a peak, the Curie temperature will have been reached. Since no peak is observed we can conclude that the Curie temperature has not yet been reached and that we must go to temperatures greater than those we observed.

4 Conclusion

After heating up the pyrrhotite sample, magnetic hysteresis was observed and the Néel temperature was determined. The Néel temperature was found by examining the non-linearity, which is the harmonic distortion, as a function of temperature. This analysis was preferred over others because a greater contrast is observed. This allows for increased accuracy and gives a Néel temperature of $597 \pm 2K$. This value agrees with the theoretical value of $598K$.

The heating of the magnetite sample wasn't completed due to technical difficulties. While the exact Curie temperature cannot be concluded from the gathered data, assumptions can be made. Since no change in magnetism occurred in any of the gathered data, we know that the Curie temperature was not obtained. This means that the Curie temperature of magnetite occurs at a value greater than that at which measurement ceased. The temperature of ceased measurement, as determined from the graph of magnetic susceptibility as a function of temperature, was found to be $702 \pm 3K$. The Curie temperature of magnetite is greater than $702 \pm 3K$, which agrees with the theoretical value of $851 K$.

References

- [1] S. Chikazumi. *Physics of Ferromagnetism*, page 28. Oxford Science Publishing, 1998.
- [2] T. Nagata. *Rock-Magnetism*, page 15. Maruzen Co., 1953.
- [3] W. Nesse. *Introduction to Mineralogy*, page 386. Oxford University Press, 2000.
- [4] C. Klein. *Mineral Science*, page 360. John Wiley and Sons, Inc., 2002.
- [5] S. Chikazumi. *Physics of Ferromagnetism*, page 118. Oxford Science Publishing, 1998.
- [6] D. Schroeder. *An Introduction to Thermal Physics*, page 339. Addison Wesley Longman, 2000.
- [7] T. Nagata. *Rock-Magnetism*, page 29. Maruzen Co., Ltd, 1953.
- [8] C. Klein. *Mineral Science*, page 383. John Wiley and Sons, Inc., 2002.
- [9] W. Nesse. *Introduction to Mineralogy*, page 110. Oxford University Press, 2000.
- [10] D. Halliday et al. *Fundamentals of Physics*, page 928. John Wiley and Sons, 1993.

- [11] P. Tipler. *Physics: For Scientists and Engineers*, page 911. W.H. Freeman and Company, 1999.
- [12] D. Halliday et al. *Fundamentals of Physics*, page 858. John Wiley and Sons, 1993.
- [13] N. Ida. *Engineering Electromagnetics, Second Edition*, page 632. Springer-Verlag New York, 2004.
- [14] A. H. Haddad. *Probabilistic System and Random Signals*, pages 409–411. Pearson Prentice Hall, 2006.
- [15] T. Nagata. *Rock-Magnetism*, page 51. Maruzen Co., Ltd, 1953.
- [16] *Labmaster DMA Handbook*, pages 13–3. Scientific Solutions Inc., 1987.
- [17] Ashcroft and Kermin. *Solid State Physics*, page 702. Sauders College, 1976.